

## Experimental and Numerical Investigations on Dynamic Mechanical Properties of TPMS Structures

Deepak Kumar Pokkalla<sup>1\*</sup>, Brandon Turner White<sup>2</sup>, Jier Wang<sup>3</sup>, Ryan Spencer<sup>2</sup>, Ajit Panesar<sup>3</sup>,  
Seokpum Kim<sup>1</sup> and Uday Vaidya<sup>2</sup>

<sup>1</sup>Manufacturing Science Division, Oak Ridge National Laboratory, TN 37932, USA

<sup>2</sup>Tickle College of Engineering, University of Tennessee, Knoxville, TN, 37916, USA

<sup>3</sup>Department of Aeronautics, Imperial College London, SW7 2AZ, UK

\*Corresponding author: [pokkallad@ornl.gov](mailto:pokkallad@ornl.gov)

### Abstract

Triply Periodic Minimal Surface (TPMS) lattice structures have been of increasing interest due to their light weighting, enhanced mechanical properties, and energy absorption characteristics for automotive and biomedical applications. With the advent of additive manufacturing and geometric modeling software, TPMS lattices with complex geometries can be realized. In this work, TPMS lattice structures were fabricated with PLA using fused filament fabrication (FFF) and their dynamic properties are characterized through drop tower experiments. Although lightweight TPMS lattices are beneficial for their impact absorption capability, most of the existing works are limited to quasi-static compression, and dynamic impact tests are rarely performed. The current study investigates the stress-strain and energy absorption characteristics of TPMS lattices through drop tower testing and numerical modeling. Finite element modeling for TPMS lattices is carried out to validate the experimental responses. The mechanical properties, deformation, and failure mechanisms of TPMS lattices under dynamic impact are summarized for potential future applications.

### Introduction

In recent years, lattice structures have gained popularity due to their light weighting, enhanced mechanical properties such as energy absorption, and thermal management capabilities for automotive, aerospace, and biomedical applications [1-4]. With the advent of additive manufacturing, a range of lattice structures in custom and complex shapes can be realized. Incorporating these lattice structures into traditional components to reduce weight is becoming increasingly feasible with readily available software like *nTopology*, *Altair*, and *Materialise*. For instance, lattice structures can be used in orthopedic implants as scaffolds for bone and tissue regeneration [5-6]. Lattice cores can be used in industrial heat exchangers to improve their efficiency [7].

The selection of a suitable lattice for a given application is often a cumbersome task given the vast array of lattice structures, despite classifying them majorly into volumetric or surface-based and periodic, non-periodic, or stochastic lattices [8]. The lattice type, size, material, and manufacturing process can drastically change the mechanical or thermal response of the overall lattice-based structural component [3-4,9]. Hence, it is essential to choose the appropriate lattice structure with geometrical features and material to achieve desired mechanical properties for industrial applications.

\* This manuscript has been authored in part by UT-Battelle, LLC, under contract DE-AC05-00OR22725 with the US Department of Energy (DOE). The US government retains and the publisher, by accepting the article for publication, acknowledges that the US government retains a nonexclusive, paid-up, irrevocable, worldwide license to publish or reproduce the published form of this manuscript, or allow others to do so, for US government purposes. DOE will provide public access to these results of federally sponsored research in accordance with the DOE Public Access Plan (<http://energy.gov/downloads/doe-public-access-plan>).

Among various lattice structures, the triply periodic minimum surface (TPMS) lattices have been gaining interest due to their high strength and energy absorption characteristics [10]. TPMS lattices are also known for carrying more loads and producing smoother crushing because of more uniform stress distributions [11]. Despite the advantages of the TPMS lattice structures, such as high energy absorption, most of the existing studies for composite TPMS lattices are limited to studying the elastic or quasi-static mechanical responses [3]. Various functional gradients such as density and cell size have also been introduced to evaluate the effect of tailored designs on the compression responses of TPMS lattices [4]. To this end, this work focuses on evaluating the dynamic mechanical responses of the polymer TPMS lattices, specifically gyroid and diamond, for different impact velocities.

Finite element analysis is commonly used for the numerical evaluation of the mechanical properties of lattices structures [12-14]. Several finite element-based optimization frameworks have also been developed for the design of lattice structures to achieve prescribed mechanical responses over large strains [15-16]. In addition, several different strategies can be used to model these TPMS lattices such as shell, solid, and voxel models. The choice of an appropriate model depends on the accuracy, computational efficiency, ease of modeling, and is often considered as a trade-off from one another. For TPMS lattices, voxel models with hexahedral finite element meshes have shown potential to provide accurate mechanical property predictions with high computational efficiency [3]. Hence, gyroid and diamond lattice structures were modelled through voxels for the numerical simulations in this work.

### **Fabrication and Experiments**

The TPMS lattices are surface-based lattice topologies that can be described using mathematical equations. Gyroid (G) and diamond (D) lattices can be generated with the prescribed number of unit cells and volume fraction from the following equations.

$$C_G = \cos(X) * \sin(Y) + \cos(Y) * \sin(Z) + \cos(Z) * \sin(X) - t$$

$$C_D = \sin(X) \sin(Y) \sin(Z) + \sin(X) \cos(Y) \cos(Z) + \cos(X) \sin(Y) \cos(Z) + \cos(X) \cos(Y) \sin(Z) - t$$

where  $X, Y$ , and  $Z$  are given by  $\frac{2*\pi*k}{L}$  with  $k$  and  $L$  prescribing the number of unit cells and length of the structure in each direction. The volume fraction of the lattice structure can be tuned using the parameter  $t$ . The change in volume fraction within the unit cells could result in vastly different mechanical responses of these lattice structures.

In this work, gyroid and diamond lattices were chosen and their mechanical responses under dynamic loading were investigated. The geometries for these lattices with 50% volume fraction in a configuration of 7 x 7 x 7 that fit into a 40 mm side cube were generated using the above mathematical equations and the corresponding STL files were generated as shown in Fig. 1. The STL files were sliced in Ultimaker Cura with an infill density of 100%, a standard quality layer height of 0.2 mm, a printing temperature of 210 °C, and a print speed of 80.0 mm/s. Four specimens of gyroid and three specimens of diamond lattice were manufactured using PLA with an Ender 3 Pro desktop 3D printer. The printed gyroid and diamond lattice structures are depicted in Fig. 2.

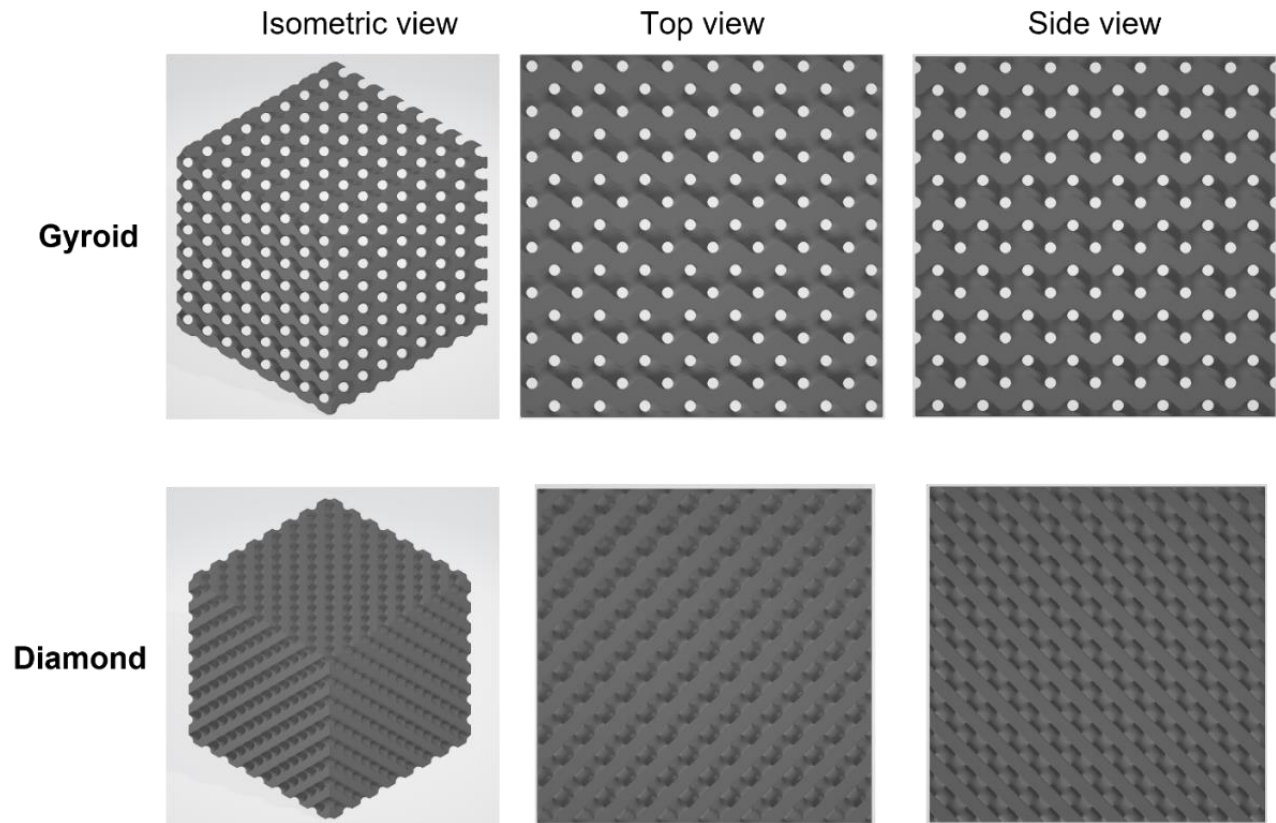


**Figure 1:** As designed TPMS lattice structures (gyroid and diamond) with a configuration of 7 x 7 x 7-unit cells in a side length of 40 mm and 50% volume fraction.

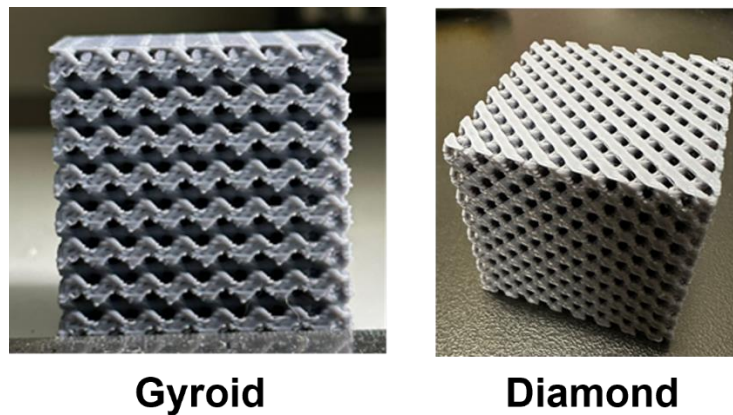


**Figure 2:** As printed TPMS lattice structures using PLA with an Ender 3 Pro desktop 3D printer.

The total mass of the printed lattice blocks was measured and averaged to obtain a total mass of 35.74 g and 34.79 g for gyroid and diamond lattices, respectively. The side length of the lattice cubes was also measured to be approximately 40 mm. These fabricated specimens were subjected to dynamic impact testing using a drop tower shown in Fig. 3.

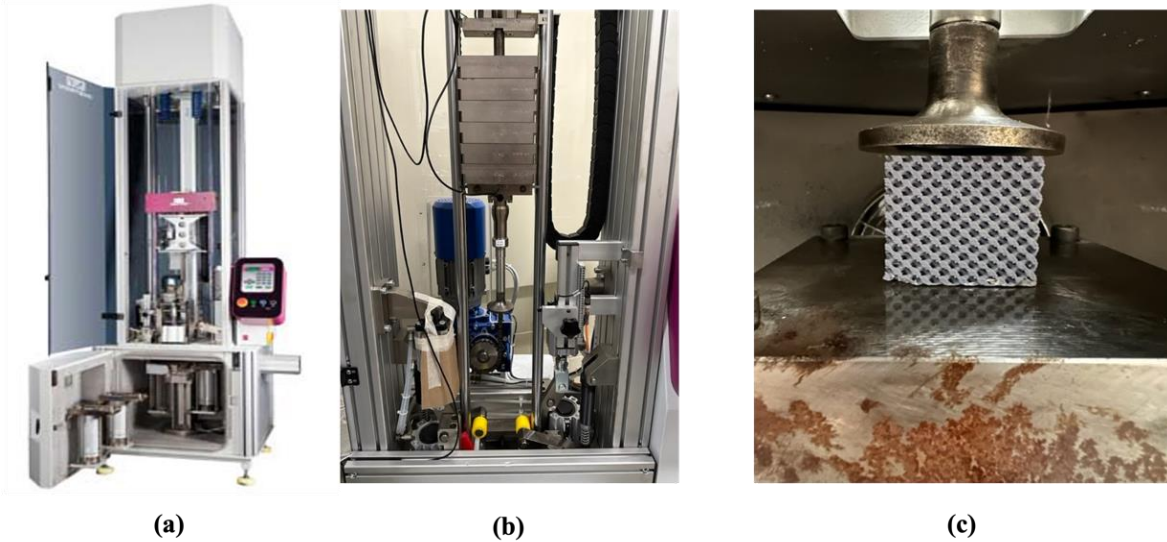


**Figure 3:** (a) Intron CEAST 9340 Drop Tower, (b) Setup with 22kN tup, six 5 kg load cells, and 60 mm flat tup head, and (c) Setup with tup height set.

The Instron CEAST 9340 drop tower (refer Fig. 3(a)) was used for drop tower experiments in this work. The CEAST data acquisition system measures the force (N), energy absorption (J), and displacement (mm) using the kinetic energy equation based on the predetermined drop height and velocity. A 22kn tup head was used for the data acquisition with a 60 mm  $\varnothing$  flat tup head, and the overall mass of impact was set to 33.215 kg, which has a base standard weight tup holder (7510.021) mass of 3.215kg with an additional mass of 30kg as shown in Fig. 3(b). The data acquisition system used was the CEAST DAS 64k - SC High Speed Data Acquisition Unit (7191.000). The parameters for the experiment were set to a frequency of 2000kHz and 64,000 data points with a working force range of 31kN. Each experiment complied with ASTM D7136 standard test type.

For the experimental setup, the adjustable height stand (7520.035) below the 3D structure was adjusted so that the lowest point of the flat tup-head could only reach the third from the bottom layer of each lattice block so that no damage could occur to that region and avoids hitting the metallic fixture. Before the test could initiate the tup-head's position was adjusted to slightly above the top of the lattice structure, as seen in Fig. 2(c), and the laser for when the data acquisition begins is set to that height. The 3D structure must be centered relative to the tup-head, and once centered, the drop test can be initiated.

Each specimen test was conducted at a constant velocity of 4.5 m/s and impact height of 1032 mm. The 30kg constant mass was determined to induce sufficient deformation in the specimens based on the preliminary tests conducted with weights of 5kg, 10kg, 20kg, 25kg, and 30kg. The samples in each preliminary test conducted were evaluated for any visual damage along with their force-time graphs. Upon these preliminary experiments, a constant weight of 30 kg is used subsequently for testing the gyroid and diamond lattice structures.

### **Numerical Simulations**

Modelling and finite element simulations are beneficial for rapidly evaluating the mechanical properties of various TPMS lattice structures with different volume fractions and geometrical features. In this work, finite element analysis on lattice structures was performed using ABAQUS/Explicit solver. There are several different meshing strategies that can be explored for surface-based lattice structures such as shell, solid, and voxel models. Depending upon the geometry and the volume fractions, these models provide a trade-off between the accuracy, modelling ease and efficiency, and data management.

In this work, a gyroid lattice structure with 7x7x7 unit cells (side length of 40 mm) and 50% volume fraction is meshed using a voxel model following the procedure presented in [3] and as shown in Fig. 4. The gyroid lattice was placed on a lower fixed rigid plate and the impactor is modeled as a top rigid plate. The top impactor with a weight of 30 kg hits the lattice structure at a velocity of 4.5 m/s. A nonlinear elastic-plastic material model calibrated from the uniaxial test data on PLA [17] is used for material model here. The elastic modulus of the PLA is determined to be 2554.7 MPa and an elastic Poisson's ratio of 0.33. A non-linear isotropic hardening is used in the plastic region. The rate-dependency of the PLA is ignored in this current study as the variation in elastic modulus for small impact velocities up to 4.5 m/s is found to be small from the dynamic mechanical analysis. Modelling the strain-rate dependency effects for accurate estimation of the mechanical properties of the lattice structures subjected to high-rate impacts is part of our ongoing work.

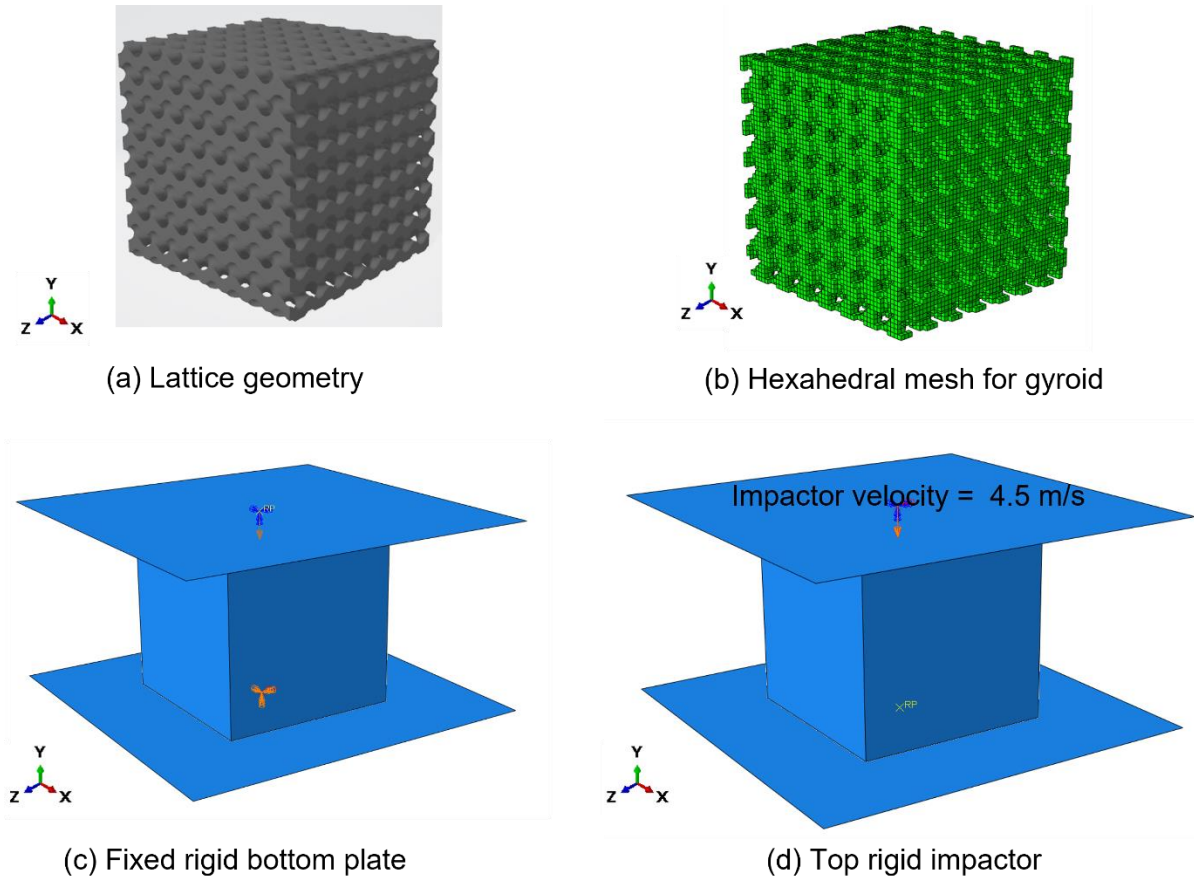


**Figure 4:** (a) Gyroid lattice structure with 7x7x7 unit cells and 50% volume fraction, (b) Hexahedral finite element mesh with C3D8R elements, (c-d) Boundary conditions – fixed bottom rigid plate and top plate impacting at a velocity of 4.5 m/s.

The modeling approach for the voxel model is adopted from [3], where surface-based geometry of the TPMS lattice is converted into a 3D array that was mapped directly to a hexahedral mesh with C3D8R elements. A 3D uniform mesh is embedded to encompass the lattice geometry where the voxels mapped to the solid material and voids can be easily distinguished. The errors associated with the voxel-based mesh discretization were alleviated by performing a mesh refinement study and choosing the appropriate resolution that provides converged mechanical responses. Python scripts were developed to generate the voxel models and assign the material properties, boundary conditions, and analysis steps automatically once the type of lattice, volume fraction, and voxel resolution are chosen. Finite element analyses on gyroid lattice structures with various numbers of unit cells and volume fractions were performed. The numerical model developed will be compared with the experiments in the next section for validation, and the next steps are outlined.

## Results and Discussion

In this section, the experimental and numerical results on the dynamic mechanical properties of the gyroid and diamond TPMS lattice structures are presented. The drop tower tests were first performed on a set of gyroid samples with different drop weights to determine the weight that would induce large strains. The samples selected consist of 7x7x7 unit cells and the overall dimensions of the cube are 40 mm x 40 mm x 40 mm. During the drop tower experiments, the force is measured from the sensors at the top of the tup. The corresponding stress is determined by dividing the measured force by the top cross-sectional area of 40 mm x 40 mm. Similarly, the effective strain is measured as the ratio of the top displacement to the original height of the lattice as 40 mm.

Preliminary investigations on gyroid samples with various weights indicated that a drop weight of 30 kg would induce large strains in the specimens. Hence, the drop tower impact tests are performed on four gyroid specimens with the same drop weight of 30 kg and the corresponding stress-strain curves were extracted as shown in Fig. 5(a). These lattices boast enhanced energy absorption capabilities and thus, the energy absorbed with time of the drop tower impact tests were plotted in Fig. 5(b). All four tests showed good repeatability and the gyroid lattice is shown to absorb up to 250J of energy.

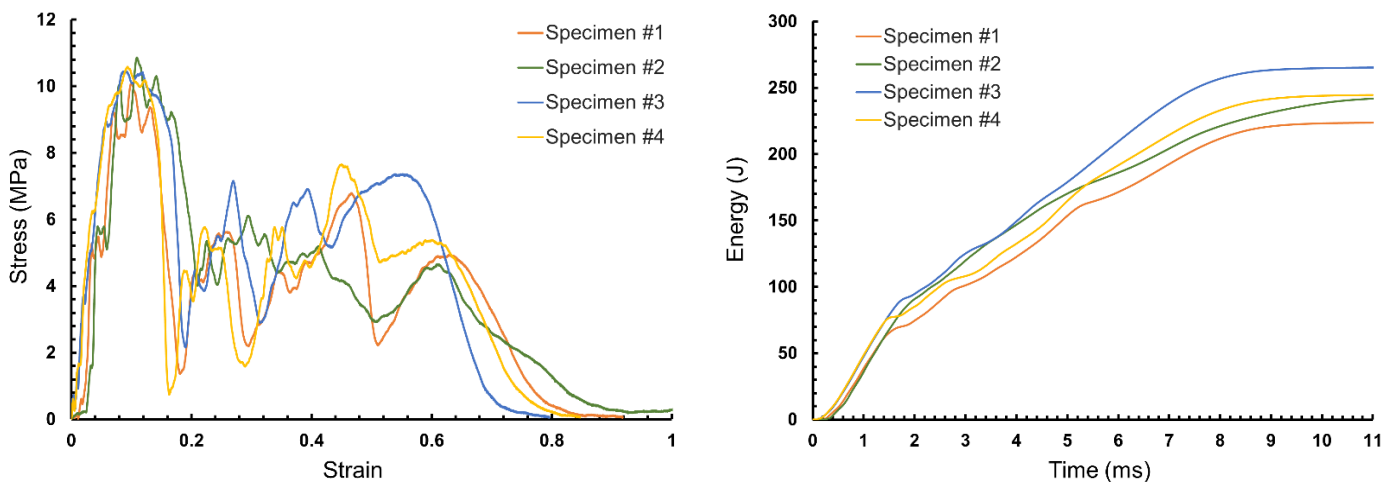


**Figure 5:** Dynamic mechanical response of gyroid lattices for an impact velocity of 4.5 m/s and drop weight of 30 kg: (a) Stress-strain curves, and (b) Energy absorption characteristics of four specimens with 50% volume fraction.

Next, a diamond lattice structure was chosen, and the drop tower tests were repeated on it with the same 30kg drop weight. The stress-strain curves and the energy absorption plots are depicted in Fig. 6(a) and (b), respectively. It is evident that the 1<sup>st</sup> peak stress of 16.5 MPa occurs around 10% strain for diamond lattice whereas for gyroid the 1<sup>st</sup> peak stress value is 10.5 MPa. Comparing the energy absorption plots in Fig. 5(b) and Fig. 6(b) reveals that the energy absorption observed under dynamic impact in case of diamond lattices are more due to the higher peaks and valleys in the stress-strain curves.

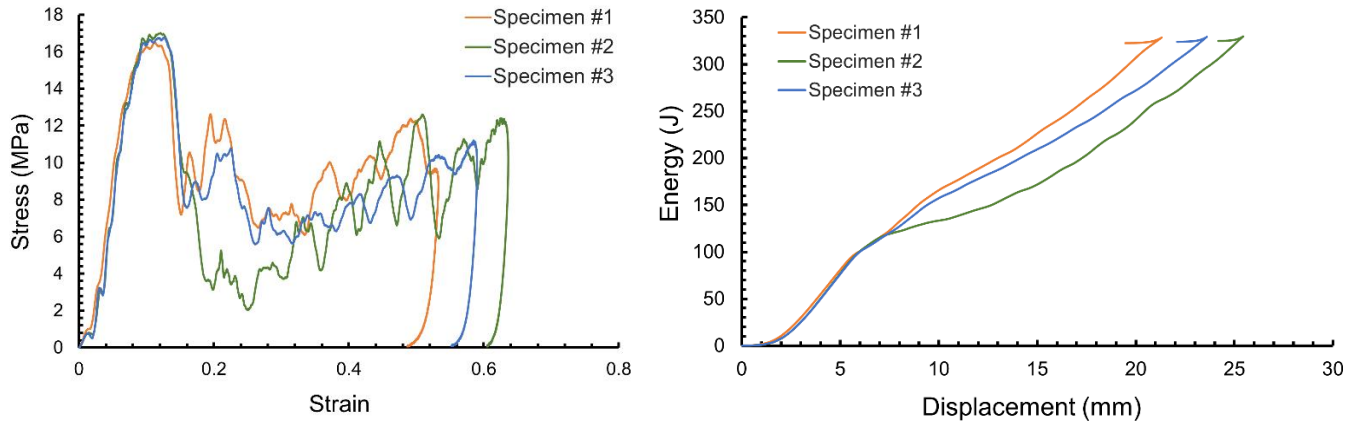


**Figure 6:** Dynamic mechanical response of diamond lattices for an impact velocity of 4.5 m/s and drop weight of 30 kg: (a) Stress-strain curves, and (b) Energy absorption characteristics of four specimens with 50% volume fraction.

Dynamic explicit finite element simulations were performed on voxel model for the gyroid lattice structure and compared with the average stress-strain response obtained from the experiments as shown in Fig. 7. The dynamic explicit numerical simulation with mass scaling predicted the dynamic elastic modulus accurately, however, overpredicted the transition to the nonlinear regime. The voxelized model is overpredicting the stiffness as the voxels corresponding to void region are modelled with low elastic modulus instead of removing them completely. The von Mises stress contours for the gyroid unit cells during the dynamic impact are shown in Fig. 8. The compression and high stresses occur at the critical locations within the unit cells and propagate throughout the geometry with further impact. This indicates that more elements are subjected to higher stress with impact, until final failure occurs due to damage.

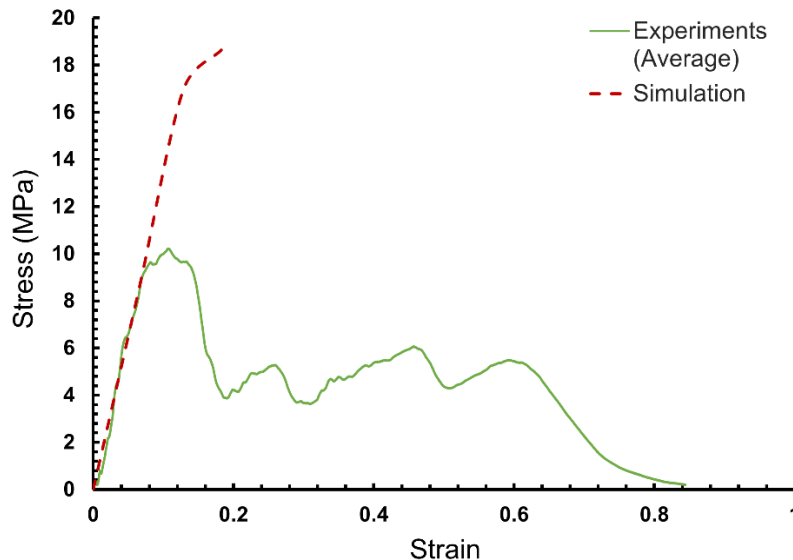


**Figure 7:** Comparison of numerical stress-strain response with average response from the drop tower experiments for an impact velocity of 4.5 m/s and drop weight of 30 kg.

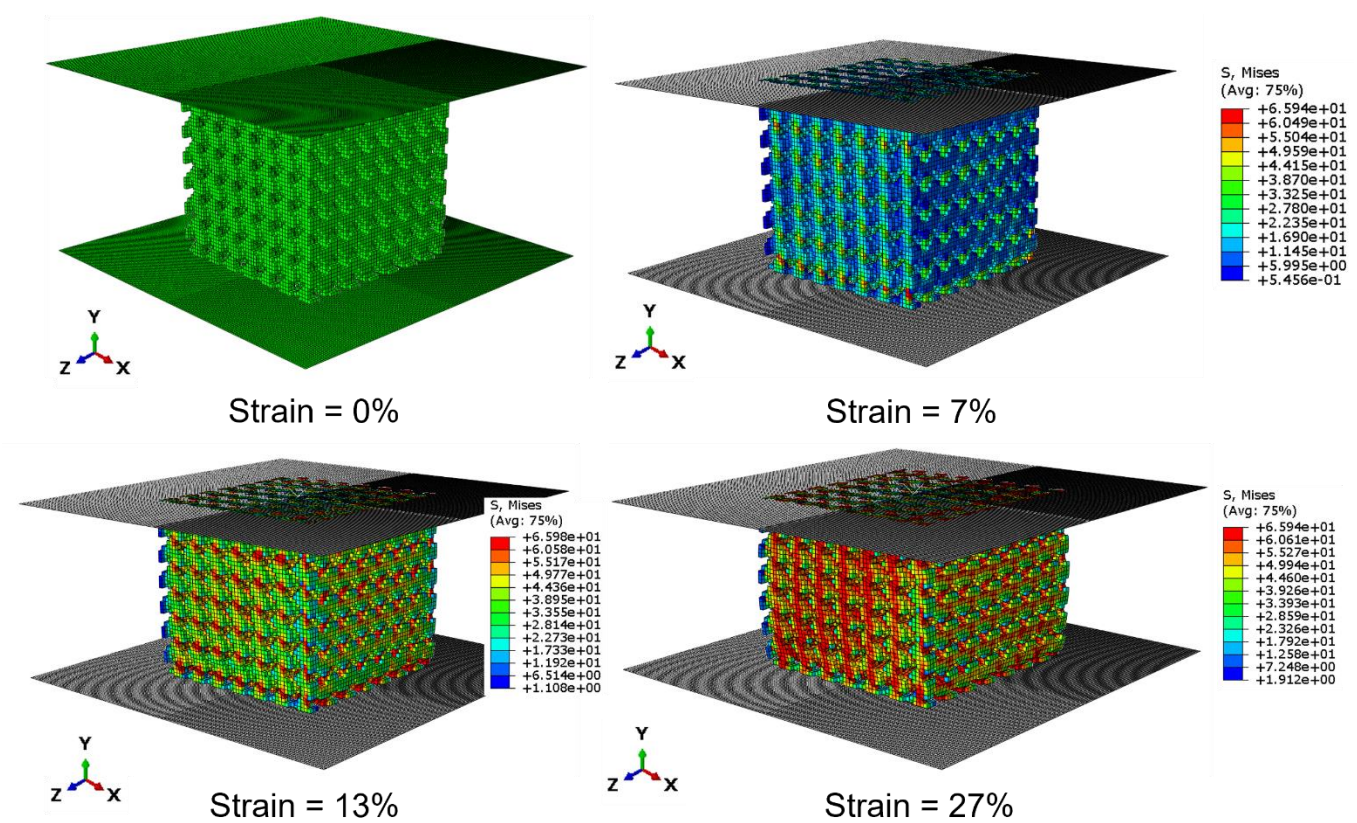


**Figure 8:** Resultant von Mises stress contours for the gyroid lattice structure subjected to impact at 4.5 m/s velocity with a 30 kg impactor.

## Conclusion

In this paper, the mechanical properties of two TPMS lattice structures, namely gyroid and diamond under dynamic compression, were systematically investigated. The lattice structures were first printed using PLA in a desktop printer with enough unit cells within overall dimensions prescribed by the drop tower experimental setup. The response of the lattice structures under different drop weights was first studied and 30 kg drop weight was selected for further investigation. The stress-strain and energy absorption characteristics of gyroid and diamond lattices under drop tower impact with the same drop weight were experimentally determined. It was evident that diamond lattices undergo higher 1<sup>st</sup> peak stress than gyroid lattices under dynamic impact and thus have better energy absorption capability overall. A voxelized dynamic explicit numerical model was further developed to evaluate the mechanical response of the gyroid lattice. The comparison of numerical results with experiments revealed that the numerical predictions lead to stiffer response. One possible reason is that the voxels corresponding to void are not removed in the numerical model, instead small modulus values were assumed. Further development of the numerical model to match the experimental results and in-depth investigation of damage and failure mechanisms in TPMS lattice structures is part of our ongoing work.

## Acknowledgments

The research is in part supported by the US Department of Energy (DOE), Office of Energy Efficiency and Renewable Energy, Advanced Manufacturing Office, under contract DE-AC05-00OR22725 with UT-Battelle LLC.



## References

1. Ashby, M.F., Evans, T., Fleck, N.A., Hutchinson, J.W., Wadley, H.N.G. and Gibson, L.J., 2000. *Metal foams: a design guide*. Elsevier.
2. Al-Ketan, O., Lee, D.W., Rowshan, R. and Al-Rub, R.K.A., 2020. Functionally graded and multi-morphology sheet TPMS lattices: Design, manufacturing, and mechanical properties. *Journal of the mechanical behavior of biomedical materials*, 102, p.103520.
3. Maskery, I., Sturm, L., Aremu, A.O., Panesar, A., Williams, C.B., Tuck, C.J., Wildman, R.D., Ashcroft, I.A. and Hague, R.J., 2018. Insights into the mechanical properties of several triply periodic minimal surface lattice structures made by polymer additive manufacturing. *Polymer*, 152, pp.62-71.
4. Plocher, J. and Panesar, A., 2020. Effect of density and unit cell size grading on the stiffness and energy absorption of short fibre-reinforced functionally graded lattice structures. *Additive Manufacturing*, 33, p.101171.
5. Guo, X., Zheng, X., Yang, Y., Yang, X. and Yi, Y., 2019. Mechanical behavior of TPMS-based scaffolds: a comparison between minimal surfaces and their lattice structures. *SN Applied Sciences*, 1(10), p.1145.
6. Melchels, F.P., Bertoldi, K., Gabbriellini, R., Velders, A.H., Feijen, J. and Grijpma, D.W., 2010. Mathematically defined tissue engineering scaffold architectures prepared by stereolithography. *Biomaterials*, 31(27), pp.6909-6916.
7. Alteneiji, M., Ali, M.I.H., Khan, K.A. and Al-Rub, R.K.A., 2022. Heat transfer effectiveness characteristics maps for additively manufactured TPMS compact heat exchangers. *Energy Storage and Saving*, 1(3), pp.153-161.
8. <https://www.ntop.com/resources/blog/guide-to-lattice-structures-in-additive-manufacturing/>
9. Kim, S., Nasirov, A., Pokkalla, D.K., Kishore, V., Smith, T., Duty, C. and Kunc, V., 2023. Compression and energy absorption characteristics of short fiber-reinforced 2D composite lattices made by material extrusion. *Engineering Reports*, p.e12701.
10. Yoo, D.J., 2015. New paradigms in cellular material design and fabrication. *International Journal of Precision Engineering and Manufacturing*, 16, pp.2577-2589.
11. Al-Ketan, O., Rowshan, R. and Al-Rub, R.K.A., 2018. Topology-mechanical property relationship of 3D printed strut, skeletal, and sheet based periodic metallic cellular materials. *Additive Manufacturing*, 19, pp.167-183.
12. Kladovasilakis, N., Tsongas, K. and Tzetzis, D., 2021. Mechanical and FEA-assisted characterization of fused filament fabricated triply periodic minimal surface structures. *Journal of Composites Science*, 5(2), p.58.
13. Afshar, M., Anaraki, A.P. and Montazerian, H., 2018. Compressive characteristics of radially graded porosity scaffolds architected with minimal surfaces. *Materials Science and Engineering: C*, 92, pp.254-267.
14. Pokkalla, D.K., Poh, L.H. and Quek, S.T., 2021. Isogeometric shape optimization of missing rib auxetics with prescribed negative Poisson's ratio over large strains using genetic algorithm. *International Journal of Mechanical Sciences*, 193, p.106169.
15. Pokkalla, D.K., Wang, Z.P., Poh, L.H. and Quek, S.T., 2019. Isogeometric shape optimization of smoothed petal auxetics with prescribed nonlinear deformation. *Computer Methods in Applied Mechanics and Engineering*, 356, pp.16-43.
16. Pokkalla, D.K., Wang, Z., Teoh, J.C., Poh, L.H., Lim, C.T. and Quek, S.T., 2022. Soft Missing Rib Structures with Controllable Negative Poisson's Ratios over Large Strains via Isogeometric Design Optimization. *Journal of Engineering Mechanics*, 148(11), p.04022063.
17. Brischetto, S. and Torre, R., 2020. Tensile and compressive behavior in the experimental tests for PLA specimens produced via fused deposition modelling technique. *Journal of Composites Science*, 4(3), p.140.